14th Australasian Fluid Mechanics Conference
Adelaide University, Adelaide, Australia
10-14 December 2001

Interpretaion of space-time correlation measurements in light of the attached eddy hypothesis

A. K. Mesbah Uddin[1], Ivan Marusic[2] and P. K. Subareddy[2]

[1]Department of Mechanical Eginerring
BUET, Dhaka 1000, BANGLADESH
[2]Department of Aerospace Engineering & Mechanics
University of Minnesota, Minneapolis, MN 55455, USA

Abstract

Two point space-time correlation of velocity fluctuations in a turbulent flow has long been viewed as containing a wealth of information as to the geometric and statistical structure of eddies in a turbulent flow. In this paper an attempt is made to interpret these measurements in light of Townsend's attached eddy hypothesis. Both numerical (DNS) and experimental data is considered. The experiments were carried out at two different Reynolds numbers in order to interpret the Reynolds number effects in terms of the eddy geometry. A simulation based on the attached eddy hypothesis tests the conjecture for certain geometrical and dynamical properties of the constituent eddies, by comparing the statistics gathered from experiment and DNS.

Introduction

Two point space-time correlations of velocity fluctuations in a turbulent flow have long been viewed as a potential tool for the eduction of the organized events or the *coherent structures*. The research community are of diversified opinion as to the exact definition of *coherent structures* and the details of their geometric, kinematic and dynamic characteristics. In fact, though an eddy is intuitively a clear concept yet expressing this within the rigors of an unambiguous formal definition seems to be a daunting task. In spite of this, the prevailing common consensus is that they play the most dominant role in transport phenomenon in a turbulent flow. Two point space-time velocity correlations play a major role in exploring various statistical aspects of these structures. Various techniques, such as POD, stochastic estimation of single point, two-point correlation tensors etc. have been proposed for exploiting this wealth of information in interpreting the results in terms of structure geometry and dynamics. In this paper various aspects of the correlation measurements were examined in light of the attached eddy model of wall turbulence, first proposed by [9] and, later, realized into a phenomenological model by [6] (hereinafter will be referred to as PC1). Since then this model has been scrutinized and refined by Perry & coworkers ([5]) and the model was found to be successful as a means of providing a framework in which to interpret the mean statistics in wall turbulence. However, these works were primarily confined to the single point statistics like mean velocity, Reynolds stresses and spectra. The major aim of this paper is to interpret two point statistics in the spirit of the attached eddy model.

Starting from the equations of motion, [8], with some intuitive arguments, proposed that a turbulent shear flow consists of geometrically similar *horseshoe-vortices* with representative dimensions proportional to their distance from the boundary and inclined in the flow-direction at an average angle of 45^0. Later [3] showed by very convincing flow-visualization studies with smoke that a turbulent boundary layer appears to consist of a 'forest' of hairpin vortices which lean in the downstream direction at approximately 45^0. These vortices may loosely be termed *coherent attached eddies* or simply *eddies*. As stated earlier, many definitions for the term coherent structure or coherent eddy exist, however, for the purpose of the current investigation, eddies will be regarded as structures having similar recognizable patterns with an angle of inclination relative to the wall. Recent studies of Adrian and coworkers, using high resolution planar PIV measurements ([2], [1]) have revealed that the boundary layer is thickly populated with hairpin vortices which occur in groups (*packets*) with a definite spatial arrangement within the group, one behind the other forming coherent packets of vortices, which occur through out the outer region in a hierarchy of scales. In spite of minor differences in the detailed interpretations, this can be regarded as the most convincing experimental evidence as to support the arguments of the attached eddy model. In a complementary computational work, [4] showed that by incorporating the scenario of packets into the attached eddy model, some temporal statistics observed in a boundary layer can be validated. [2] showed with their PIV data how the structural information contained in the two-point correlation can be associated with the presence of hairpin vortex packets. In this paper, a full account of both experimental and computational investigation will be presented in order to explain the characteristics of various aspects of two point correlation measurements which include the Reynolds number dependence of these statistics as well as the geometrical structure of the eddies.

The Experiment

We will assume x, y and z as the stream-wise, cross-stream or span-wise direction and wall-normal directions respectively; while the fluctuating velocities in these directions are denoted by as u, v and w respectively. All length scales are normalized by the boundary layer thickness δ_c, if not otherwise stated, and denoted with a superscript asterisk, i.e $\ell^* \equiv \ell/\delta_c$, where ℓ is any arbitrary length scale. The experiment was carried out in a nominally zero pressure gradient open return blower type wind tunnel having a working section of 940 mm $\times$ 388 mm and a length of 4400 mm, with two normal hot-wire sensors as schematically shown in figure 1. The lower probe (close to the wall) will be referred to as the probe A, whereas the upper one as probe B. For all measurements the stream-wise separation between the probes Δx^* was kept at zero, while various wall normal separation of Δz^* were used. Two flow cases with Re_θ=4140 and 11928 were considered. With reference to figure 1, the coefficient of two-point space-time normal-

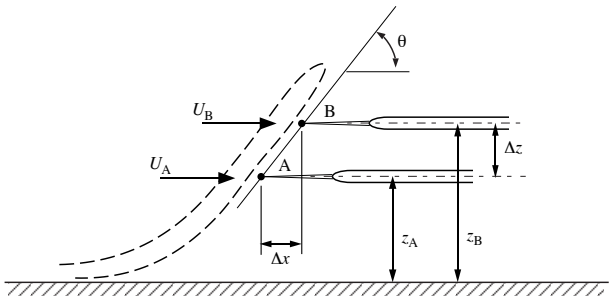

Figure 1: Definition of the terms

ized cross-correlation $\mathcal{R}_{\mathcal{AB}}$ of the fluctuating velocities at $\mathbf{A}(x_a^*, y_A^*, z_A^*)$ and $\mathbf{B}(x*_A+\Delta x^*, y_A^*+\Delta y^*, z_A^*, \Delta z^*)$, can be written as

$$\mathcal{R}_{AB}[x_A^*, y_A^*, z_A^*, \Delta x^*, \Delta y^*, \Delta z^*, \tau] = \frac{\overline{u_A\ u_B}}{\sqrt{\overline{u_A^2}}\ \sqrt{\overline{u_B^2}}} \quad (1)$$

where u_A and u_B represent the fluctuating components of the stream-wise velocities at **A** and **B** respectively and τ represents the time-shift parameter. Although the use of Taylor's hypothesis in flows with strong shear has been the issue of much debate, [10] showed that when Taylor's hypothesis is used in transforming the temporal-shift τ to the spatial-shift Δx in case of two-point correlation measurements, an inappreciable error is encountered. Now using Taylor's hypothesis, and choosing the position **A** as the origin of the coordinates system and keeping Δy^*=0 always, we can write a compacter form of (1) as

$$R_{AB}[\xi, \Delta z^*] = \frac{\overline{u_A\ u_B}}{\sqrt{\overline{u_A^2}}\ \sqrt{\overline{u_B^2}}}. \quad (2)$$

The non-dimensional parameter ξ can be defined, in terms of U_c, the convection velocity, and δ_c, as

$$\xi \ = \ \Delta x^* \ - \ \frac{\tau U_c}{\delta_c}. \quad (3)$$

For the convenience of forthcoming discussions, let the subscripts 0 and τ imply special cases of ξ corresponding to τ=0 and Δx^*=0 respectively, i.e.

$$\xi_0 = \xi|_{\tau=0} = \Delta x^*; \qquad \xi_\tau = \xi|_{\Delta x^*=0} = \frac{-\tau U_c}{\delta_c} \quad (4)$$

Note that for all calculations to come, a constant convection velocity across the entire layer with $U_c = 0.82U_1$, where U_1 is the free-stream velocity, will be used.

The Computation

In general the induced stream-wise velocity field U due to a representative eddy of scale δ and its image on the wall can be written as

$$\frac{U}{U_0} = f[\frac{x}{\delta}, \frac{y}{\delta}, \frac{z}{\delta}] \quad (5)$$

where U_0 is the characteristic velocity scale. This velocity field can be computed using Biot-Savart law and considering a Gaussian vorticity distribution within the core of the vortex filaments constituting the eddy. Let $\psi_A[k_1\delta, y/\delta, z/\delta]$ and $\psi_B[k_1\delta, y/\delta, z/\delta]$ denotes the one dimensional Fourier transform (in the stream-wise direction) of the fluctuating components of the velocity function f_A and f_B at A and B respectively. Then following the analysis given by [4], the normalized correlation R_{AB} can be written as:

$$R_{AB}[\xi_0, \Delta z^*] = \frac{\mathcal{R}'_{AB}[\xi_0, \Delta z^*]}{\sqrt{\mathcal{R}'_{AA}[0,0]\ \mathcal{R}'_{BB}[0,0]}} \quad (6)$$

where $\mathcal{R}'_{AB}$ can be defined as

$$\mathcal{R}'_{AB}[\xi_0, \Delta z^*] \ = \frac{U_0^2}{\lambda_x \lambda_y} \int_{-\infty}^{\infty}\int_{\delta_1}^{\delta_c}\int_{-\infty}^{\infty} \psi_A^*\ \psi_B\ Q^2[\tfrac{\delta}{\delta_c}] \ \times D[\tfrac{\delta}{\delta_c}]\ \tfrac{1}{\delta}\ d(\tfrac{1}{\delta})\ d\delta\ d(k_1\delta) \quad (7)$$

where the asterisk denotes a complex conjugate, and λ_x and λ_y are geometric constants relating to the random distribution of eddy length scales in the boundary layer. The limits δ_1 and δ_c denote the smallest and the largest length scales considered which are assumed to be equal to $100\nu/U_\tau$ and the boundary layer thickness respectively. The functions Q and D are weighting functions as defined in [5] where Q accounts for the variation of velocity length scale for different δ's, and D accounts for the departure of the eddy length scales distribution p.d.f from a -1 power law and how the p.d.f on the $(x, y, 0)$ surface varies with δ.

Though the numerical simulations were carried out with several simple eddy geometries, we will be restricting ourselves here to two different eddy configurations as presented in figures 2. For convenience the former one will be called a simple Π-eddy, where as the latter will be refereed to as tailed Π-eddy. The simple Π-eddy sketched in figure 2(a) consists of two predominant types of structure: there are two rods of vorticity inclined at an angle 45^0 to the downstream direction, referred to as *legs* and one span-wise rod of vorticity, the *head*. These nomenclatures are in the spirit of [7] except for the absence of the neck region connecting the head and the legs. The tailed Π-eddy in figure 2(b) contains an additional straight element, the *tail*, inclined at a shallower angle (about 17^0) than the leg in the stream-wise direction. Two different configurations of tailed Π-eddies were considered. In the first configuration a constant core radius, same as the other members, in the tail of the eddy is assumed. In the other case the core radius in the tail is allowed to vary from an infinitesimally small value at the wall to a value equal to the core radius of the other members at a plane where the leg meets the tail. Considering the experimental observation that the span-wise correlation of u_1 is confined to $\Delta y \approx \delta_c$ in the outer part of the boundary layer, as a conservative estimate, the span-wise extent of the computational domain was set to 4δ divided into 100 equally spaced grids. Note that near the wall, the experimental span-wise correlation decays to zero even earlier. The stream-wise extent of the computational box was limited to 20δ with 4096 equally spaced grid points. Based on some preliminary calculations of spectra, [5] suggested that this simple shape with $Q^2D = 1$ may be a good candidate for the representative eddy in zero-pressure-gradient boundary layer flow. In order to be consistent same assumptions are retained in the calculations to follow.

Results and Discussion

Correlation Profiles

[4] showed quite convincingly that incorporating the concept of hair-pin vortex packets of [1] in the attached eddy model, a qualitative prediction of the characteristics of auto-correlation and two-point space-time cross-correlation near the wall can be achieved. Our analysis

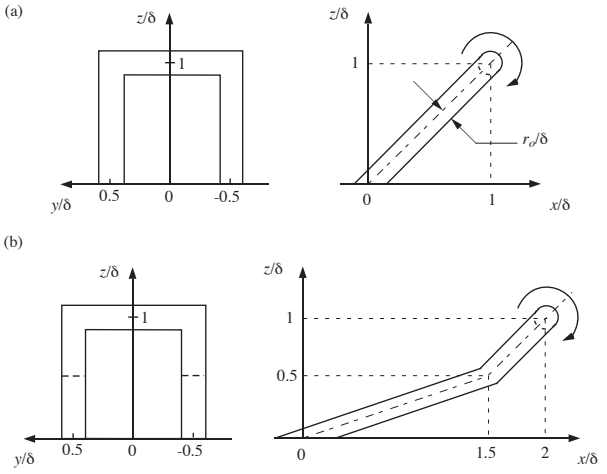

Figure 2: (a) Sketch of a simple Π eddy with its image on the wall. L_x and L_y denote the x- and y-extent of the computational box containing the eddy. (b) Sketch of a Π-shaped eddy with a one segmented tail.

on this occasion will be limited to the outer half of the boundary layer. Experimental correlation profiles at various z_A^* in the outer part of the BL corresponding to Re_θ=4140 with Δz^*=0.12, 0.15, 0.20, 0.25 and 0.30 are shown in figure 3. It can be seen that at $z_A^* \approx 0.54$, the profile with Δz^*=0.30 develops a kink which evolves into a negative peak R_{AB} at z_A*=0.77 and ultimately culminates into a Mexican Hat like appearance. Similar evolution can also be observed with the profiles corresponding to Δz^*=0.25 and 0.20, though at different z_A* while though the ultimate appearance of all of the profiles at $z_A^* \approx 1$ is more or less identical, this evolution process is not distinct with Δz^*=0.12 and 0.15. The emergence of the negative R_{AB} can be attributed to the existence of a span-wise vortex element (the head) with the probes at A and B being on the lower and upper side of the vortex. In figure 4 R_{AB} profiles computed using the attached eddy model for a range of hierarchy length scales of simple Π-eddies with $r_0* \ (r_0* \equiv r_0/\delta)$ and Δz^*=0.10 are shown with the experimental profiles corresponding to Δz^*=0.30. It can be seen that the experimental and computational profiles are going through a remarkably similar qualitative evolutions as the probe system is moved towards the edge of the BL. Simulations were carried out with a wide range of r_0^* and Δz^* and it was found that the detection of the evolution as depicted in figure 4 requires certain relationship between r_0^* and Δz^*. Based on this and from further evidence to be presented later, it appears that these two experimental and simulation cases represent comparable eddy core-radius to Δz^* ratio.

Optimum Correlation

The profiles of the optimal correlation $R_{AB}[\xi_m, \Delta z^*]$ computed using a single representative eddy length scale and a range of eddy length scales are shown in figure 5. Here ξ_m implies the value of ξ_0 when R_{AB} is maximum. One can see that in case of a single eddy length scale, there is hardly any effect of Δz for $z_A + \Delta z < \delta$. However, there is a significant Δ^z* dependence when we consider the case with a range of eddy length scales which, in fact, resembles qualitatively the experimental pattern as shown in figure 6. Comparing figures $5(a)$ and $6(a)$, we see that for Δz^* equal to 0.10 and 0.15 respectively,

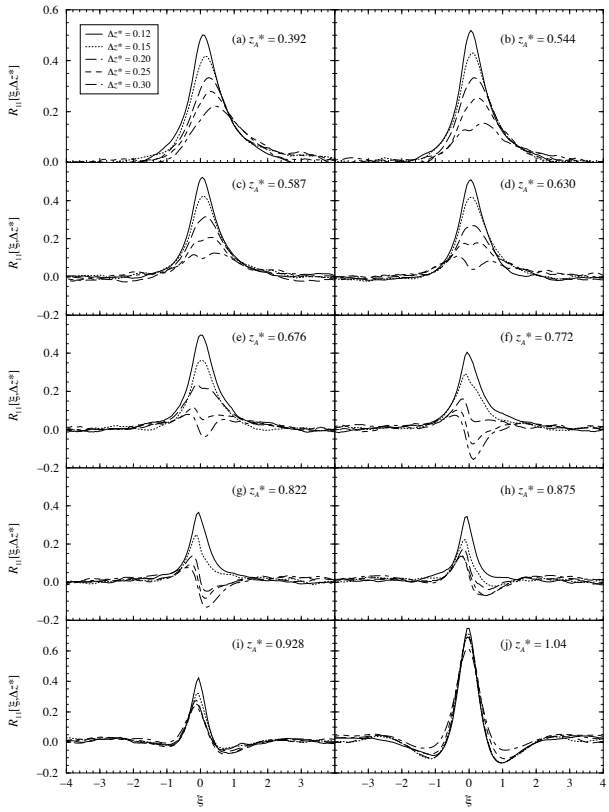

Figure 3: Effect of wall normal separation on the experimental space-time correlation profiles at Re_θ=4140

.

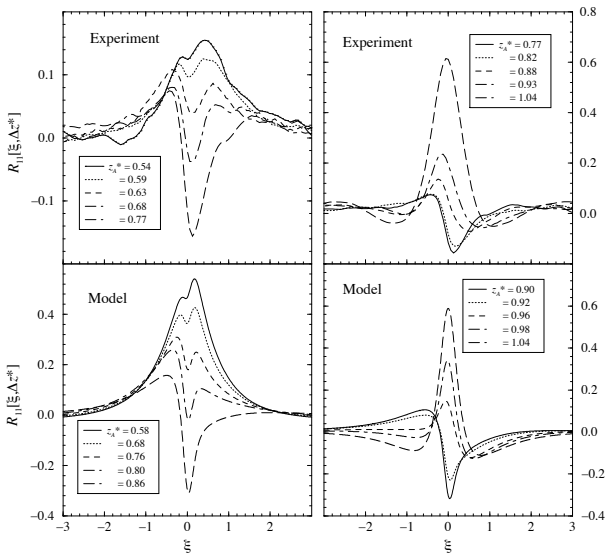

Figure 4: Trends of the experimental and computational correlation profiles in the outer part of the boundary layer. (a) Experiment with $\Delta z^* = 0.30$. (b) model with $r_0^* = 0.05$ and $\Delta z^* = 0.15$

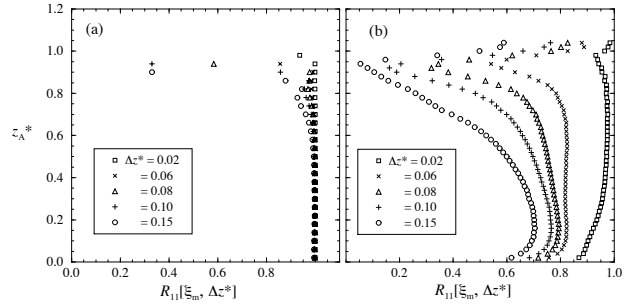

Figure 5: Dependence of the optimal correlation on the wall-normal separation for a given core radius $r_0^* = 0.05$ corresponding to (a) a single representative structure of one length scale, (b) With a range of eddy length scale distribution.

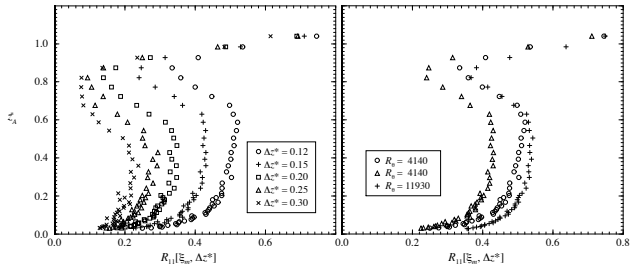

Figure 6: (a) Variation of $R_{AB}[\xi_m, \Delta z^*]$ across the boundary layer for flow G1 for different wall-normal separation Δz^*. (b) Reynolds number dependence of $R_{AB}[\xi_m, \Delta z^*]$. In all cases Δx^*=0.

the optimal R_{AB} exhibits a constant value in the middle portion of the BL. Calculations in this line using various r_0^* and Δz^* show that the appearance of this constant value occurs when we have Δz^* to r_0^* ratio of about 1. A larger ratio causes the profiles to lean forward and a smaller ratio in the other direction. Since the simulation with a single representative structure does not show up any such trend, this could be attributed to the effect of the existence of range of geometrically similar length scales. Now when the experimental optimum R_{AB} at Re_θ=11928 is considered in figure 6(b), we found that a similar profile results for a smaller Δz^* of 0.10. Now in line with the earlier observations, it can be conjectured that the eddies become skinnier as the Reynolds number is increased.

However, it is generally conceded that although we have an encouraging qualitative agreement between the experimental measurements and the simulation results, a quantitative matching is yet to be achieved.

Conclusion

References

[1] Adrian, R. J., Meinhart, C. D., & Tomkins, C. D. (2000). Vortex organization in the outer region of the turbulent boundary layer. *Journal of Fluid Mechanics* **422**, 1–54.

[2] Christensen, K. T. & Adrian, R. J. (2001). Statistical evidence of hairpin vortex packets in wall turbulence. *Journal of Fluid Mechanics* **431**, 433–443.

[3] Head, M. R. & Bandyopadhyay, P. (1981). New aspects of turbulent boundary-layer structure. *Journal of Fluid Mechanics* **107**, 297–338.

[4] Marusic, I. (2001). On the role of large-scale structures in wall turbulence. *Physics of Fluids* **3**, 735–743.

[5] Perry, A. E. & Marusic, I. (1995). A wall-wake model for the turbulence structure of boundary layers. Part 1. *Journal of Fluid Mechanics* **298**, 361–388.

[6] Perry, A. E. & Chong, M. S. (1982). On the mechanism of wall turbulence. *Journal of Fluid Mechanics* **119**, 173–217.

[7] Robinson, S. K. (1991). Coherent motions in the turbulent boundary layer. *Annu. Rev. Fluid Mech.* **23**, 601–39.

[8] Theodorsen, T. (1952). Mechanism of turbulence. In *Proc. Second Midwestern Conference on Fluid Mechanics,* The Ohio State University, March 17-19, 1952.

[9] Townsend, A. A. (1976). *The Structure of Turbulent Shear Flow.* Cambridge University Press.

[10] Uddin, A. K. Mesbah, Perry, A. E., &Marusic, I. (1997). On the validity of Taylor's hypothesis in wall turbulence. *Journal of Mech. Engg Res. and Dev.* **19-20**, 57–66.